J. Fluid Mech. (1983), *vol.* 135, *pp.* 199–217
Printed in Great Britain

A point source of heat in a stable salinity gradient

By A. B. TSINOBER, Y. YAHALOM AND D. J. SHLIEN†
Faculty of Engineering, Tel-Aviv University, Israel

(Received 29 March 1982 and in revised form 26 April 1983)

When a salinity gradient is heated at a single point, a hot plume is formed with a series of layers around and above it in a 'Christmas-tree' flow pattern. Qualitative visual observations of the development of this system are reported. Three kinds of layers are observed: the first kind is formed above the basic plume from a hierarchy of secondary plumes on top of the basic one, the second develops around the upper part of the basic plume, and is driven by the same mechanism as the layers in sidewall-heating experiments, and the third, forming around the lower part of the basic plume, is of the same nature as the second type but also has something in common with double-diffusive intrusions. A characteristic feature for all the three kinds of layers is the existence of systematic shearing motions and vortices. Quantitative estimates for the plume height and the thickness of the layers are obtained.

1. Introduction

One of the most striking features of double-diffusive phenomena in statically stably stratified fluid is the formation of systems of convecting layers separated by thin interfaces. These layers are formed under the influence of some external factor or are due to intrinsic instability arising from the destabilizing component. This property seems to be universal for double-diffusive systems and is exhibited in a great variety of situations, as reviewed by Turner (1973, 1974, 1979), Turner & Gustafson (1978), Sherman, Imberger & Corcos (1978) and Huppert & Turner (1981).

Most of the laboratory work on double-diffusive layering has been associated with solid boundaries. Turner (1968) first observed layer formation in a one-dimensional geometry in a salinity gradient heated from below, and Huppert & Linden (1979) made an extensive study of this case. Thorpe, Hutt & Soulsby (1969) observed layer formation in a salinity gradient heated from the sidewall in a narrow vertical gap, while Paliwal & Chen (1980) made a detailed study of this case for various angles of the gap inclination. Chen, Briggs & Wirtz (1971) studied layer formation in a wide gap and Huppert & Turner (1980) investigated this case in more detail.

Turner & Chen (1974) were the first to demonstrate in the laboratory the importance of horizontal gradients of T and S in the fluid interior for the formation of layers. Turner (1978) carried out an extensive study of double-diffusive intrusions, formed when water with some T, S properties intrudes at its own density level in a density gradient with different T, S properties. He showed that either a source of T‡ in a gradient of S, or a source of S in a gradient of T, split into a number of layers

† Present address: Mechanical Engineering Department, 255 Nebraska Engineering Center, University of Nebraska, Lincoln, Nebraska 68588, U.S.A.

‡ This follows the generally accepted convention of denoting the component with the higher diffusivity by T and that with the lower by S. The term 'source of T' corresponds for example, to a source of colder fresher water, and 'S-gradient' to a vertical density gradient due to S-variations.

spreading at several levels. Ruddick & Turner (1979) demonstrated the layer formation at a front across which there existed large gradients of T and S (without any horizontal density gradient). These experiments were performed in order to examine the significance of double-diffusive effects in various oceanographic contexts. An example of practically important double-diffusive effects on a buoyant plume outflow was given by Fischer (1971), in the context of sewage disposal of a cool freshwater effluent (T-source) into T-gradient of homogeneously salted water. He observed formation of a submerged cloud of salt fingers and consequently an increased vertical spread of the effluent. However, no splitting into layers was reported. Turner & Gustafson (1978) briefly reported a similar experiment on a sugar (S-source) outflow into a salinity gradient (T-gradient) (see figure 13 of their paper). They observed the splitting of the outflow into two layers. Turner & Gustafson presumed further that '. . . a multiple outflow could occur if the initial density gradient were rather weaker and the outflow stronger, so that vertical penetration was increased.'

In the work reported here we are concerned with a somewhat different case of hot saline outflow (S-source) into a salinity gradient (S-gradient, but with different T). It is produced by heating a salt-stratified fluid in a small localized region, thus producing an upflow which is warmer and saltier than its surroundings. The horizontal and vertical gradients of T and S set up in the interior of the fluid in this way lead to the formation of layers by several mechanisms which will be described. This type of flow can be regarded as a basic individual convective element, and to some extent it plays the same role in the double-diffusive convection problems as the plume in one-component convection problems. Therefore we believe that the study of this type of flow will contribute to the understanding of various double-diffusive convection problems related to heating a (homogeneous and nonhomogeneous) salinity gradient from below or from the side.

It is worth noting that in this flow it is possible to achieve a great degree of control over the important parameters using a technique proposed by Shlien & Thompson (1975). We have limited ourselves to mostly qualitative experiments at this stage, and we believe it would be premature to attempt a theoretical model before more quantitative results have been obtained.

2. The governing parameters

The system under consideration consists of a point source of buoyancy (heat) in a stably stratified (constant salinity gradient) fluid, the diffusivity of which is different from that of the injected buoyancy. This system develops in time into a complicated system consisting of a rising plume (which in our experiments was laminar), a falling annular plume around the rising one (which in our experiments was mostly turbulent) and, at later stages, of a system of double-diffusive layers which are partially turbulent and partially laminar. The physical quantities which completely specify this system are the buoyancy flux $F = Vg\Delta\rho/\rho = g\alpha Q/\rho_0 c$, the initial density gradient $N^2 = -(g/\rho_0)\,\mathrm{d}\rho/\mathrm{d}z = -g\beta\mathrm{d}S/\mathrm{d}z$, the kinematic viscosity ν, and the thermal and salinity diffusivities κ_T and κ_S respectively. Here Q is the heat flux and V the volume flux, S and ρ are the local salinity and density, ρ_0 is a reference density, α is the coefficient of thermal expansion, β the analogous coefficient for salt, c is the specific heat, g is the gravitational acceleration and z is the vertical coordinate, directed upward. These physical quantities can be reduced to three dimensionless parameters: the effective Rayleigh number $Ra = F/\kappa_T \nu N$, the Prandtl number

$Pr = \nu/\kappa_T$ and the diffusivity ratio $\tau = \kappa_S/\kappa_T$. The specification of Ra is equivalent to the more common definition of $Ra = g\alpha\Delta T l_{FN}^3/\kappa_T \nu$ with lengthscale $l_{FN} = (F/N^3)^{\frac{1}{4}}$ and temperature scale $\alpha\Delta T = \Delta\rho/\rho_0 = -(l_{FN}/\rho_0)(\mathrm{d}\rho/\mathrm{d}z)$.

In the experiments to be presented, τ and Pr remain fixed and thus the Ra-dependence will be investigated. In particular, the functional dependence f, of a height L, will be sought in the form $L = (F/N^3)^{\frac{1}{4}} f(Ra, t)$, where t is a dimensionless time such that $t = t^* N$, t^* is the actual time and L will correspond to the plume height H or a layer thickness h.

3. Apparatus, techniques and errors

Constant-salinity gradients were produced by the 'double-bucket' method, filling the $40 \times 40 \times 30$ cm high aquarium from below. Point-source heat injection was achieved by passing a 5 kHz electric current from a small electrode (1 mm diameter and 1 mm high located 55 mm from the tank bottom) to four large electrodes (6 mm diameter and 250 mm long in the four vertical corners of the tank). In this technique, described by Shlien & Thompson (1975), only the fluid near the small electrode is heated ohmically owing to the large current densities there. For each experiment the heating rate Q was maintained at a constant value between 0.41 and 17.8 W, corresponding to a range of buoyancy fluxes F, between 0.05 and 1.2 $\mathrm{cm}^4/\mathrm{s}^3$. The maximum Q was limited by bubble formation on the small electrode. The ambient relative density gradient $(1/\rho_0)(\mathrm{d}\rho/\mathrm{d}z)$ was varied from 1.4×10^{-5} to 1.2×10^{-3} cm^{-1} corresponding to N between 0.118 and 1.07 s^{-1}. The resulting values of Ra were between 2.6×10^3 and 1.36×10^5.

Shadowgraph and dye techniques were used either simultaneously or separately to observe the effects of the convection. The light source for the shadowgraph was a 15 mW He–Ne laser whose beam was filtered, expanded and collimated to 30 cm in diameter. For the dye visualization, a 3 W argon laser beam in the form of a 0.5 mm thick vertical sheet illuminated a section containing the symmetry axis. Since fluorescent dyes were used, only the dye in this section was visible. The salt solution below the electrode was tagged with Fluorescein dye (green) while vertical lines in the illuminated plane were tagged red by dropping particles of Rhodamine B in the solution. These red traces photographed orange–yellow since they were photographically overexposed.

It was found that some important details of the flow pattern were lost in the shadowgraph pictures, since the image in this case is an integrated one (of an axisymmetric pattern) along the path of the light and since the fluid density in the upper region of the layers is almost homogeneous. An example of comparison of the two techniques is given in figure 1. It is clearly seen that the vortices in the dye pictures are entirely lost in the shadowgraph one. It was also difficult to find the horizontal extent of the layers from the shadowgraph pictures, whereas in the dye photographs these were much clearer. Finally the comparison showed that the salt-finger scale is much larger than the fine scale seen in the shadowgraph. Most of the results to be presented will be based on the dye visualization.

In evaluating the flow parameters, the effect of temperature and salinity variations on fluid physical properties was neglected, leading to sizable errors for some parameters. The typical temperature increase near the source, estimated to be 10 °C, leads to the following variation of physical parameters. Pr changes from 7.0 at 20 °C to 5.4 at 30 °C. F varies by a factor of two, primarily owing to changes in thermal expansion coefficient from 1.8×10^{-4} $^\circ\mathrm{C}^{-1}$ at 20 °C to 3.2×10^{-4} $^\circ\mathrm{C}^{-1}$ at 30 °C. The

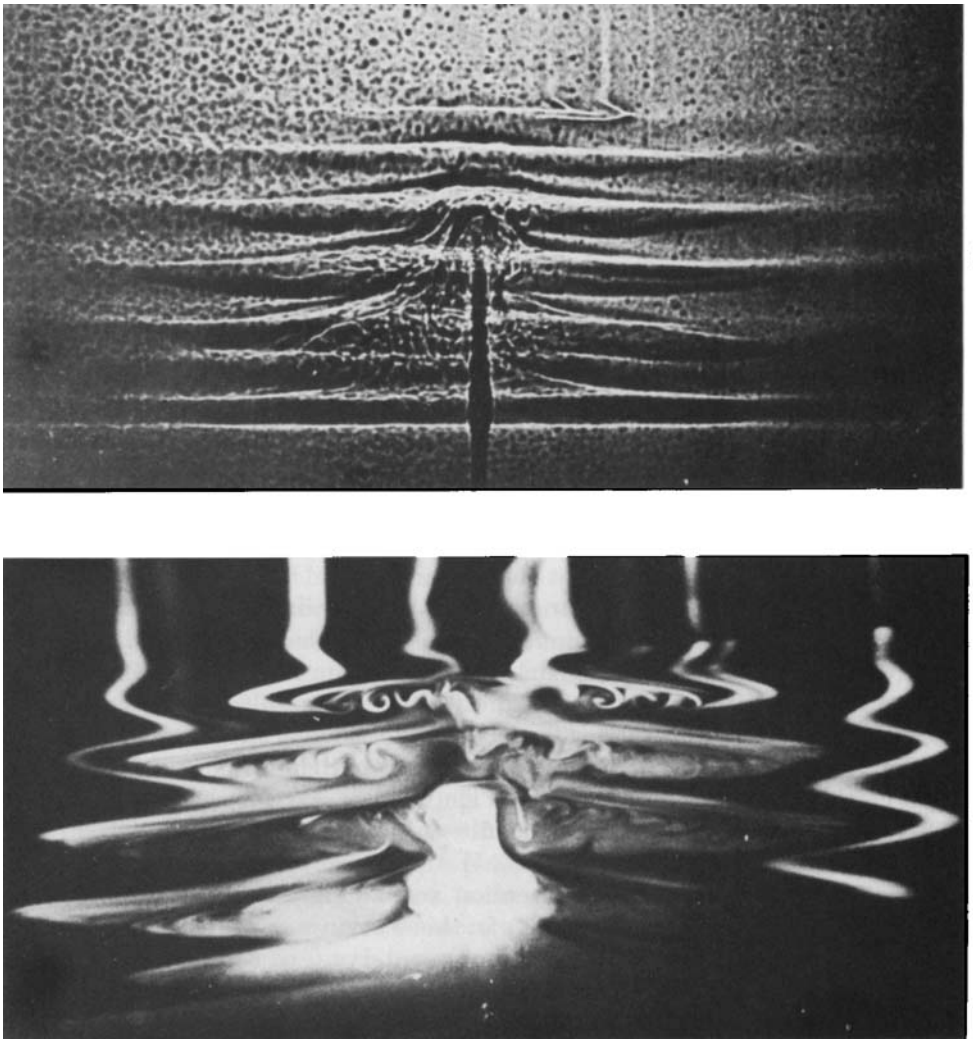

FIGURE 1. Comparison of the two visualization techniques: (*a*) shadowgraph; (*b*) dye. The two photographs were taken simultaneously at $t = 470$ s (experiment no. 1, table 1).

variation in l_{FN}, the natural lengthscale, is less than 20%; though the variation of Ra leads to more serious errors.

Because of the difficulty in defining the interface position from still photographs and from ciné film, the expected errors in the length measurement are larger than usually encountered. The error in the plume height is estimated to be up to 15%, in layer thickness, 20% and in the horizontal scale 30%.

4. Experimental results

4.1. *The initial stage*

Immediately after the heating is turned on, a vortex cap forms at the front of the starting plume as it rises. Owing to the excess of momentum the plume overshoots the level of zero buoyancy. It forms a dome on top as it reaches the maximum height,

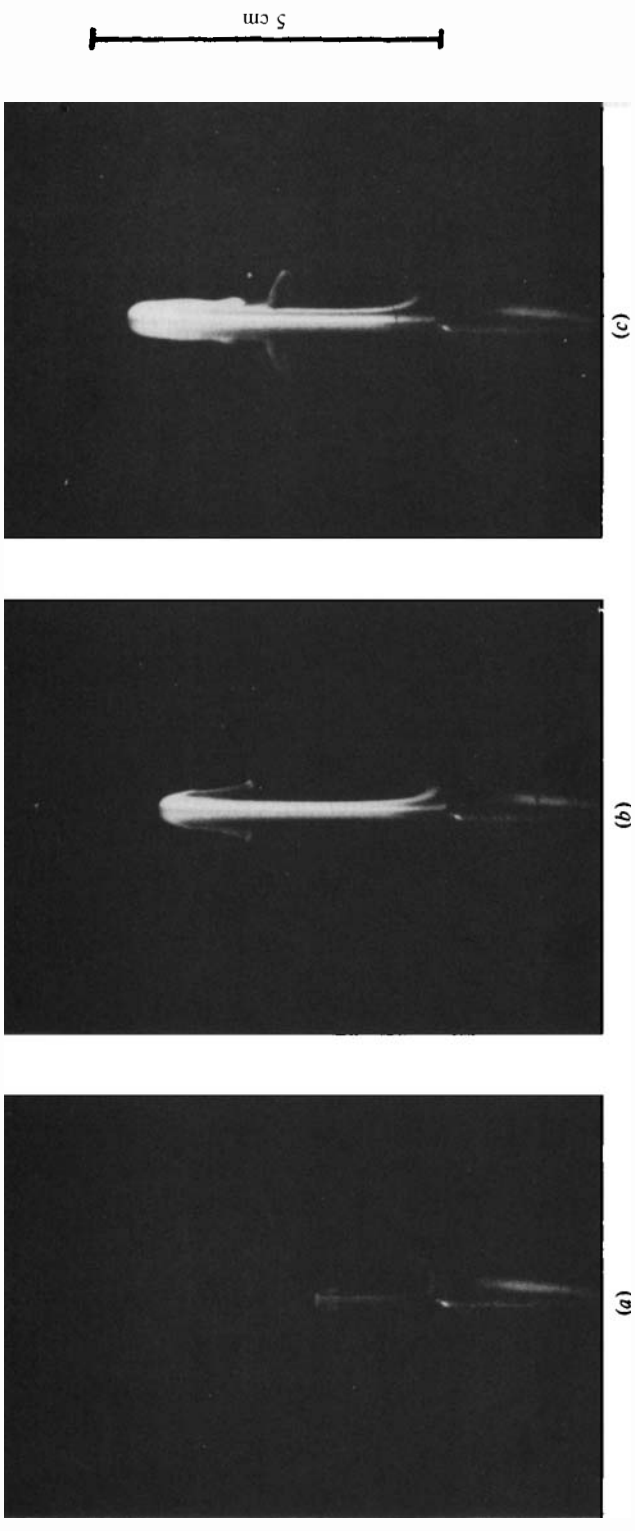

FIGURE 2. The initial stage of the plume development at $Ra = 3.11 \times 10^4$: (*a*) $t = 1.1$ s; (*b*) 6.2 s; (*c*) 11.1 s (experiment no. 3, table 1).

falls downwards in an annular region around the upflow forming a double plume structure, and then spreads out horizontally at its own density level (figure 2).

When the Rayleigh number is small enough ($Ra \approx 10^3$), the plume is laminar and the salty water raised from the heat-source level (green liquid) spreads out in one layer slightly above its original density level (figure 3). Further on, layers form successively above this one (which is warmer and more saline than the fluid above), by a mechanism similar to that extensively investigated by Huppert & Linden (1979). There are, however, some differences, since the heat flux above the first layer is non-homogeneous and decreases with the distance from the centre, resulting in a horizontal temperature gradient. Therefore the layers in our case also developed horizontally, and systematic shearing motions were set up in the layers. An important detail of the layer development could also be seen. This was the formation of vortices (rolls) near the first plume top and their slightly sloping advance into the ambient fluid. We shall return to these points later. We stress that the whole flow originates as a result of heating at a point source of heat, as is seen from figure 3. At a slightly larger heating rate, the fluid rising from the heat source level splits into two layers but the annular plume still remains laminar.

When the heating rate is large enough ($Ra \gtrsim 2 \times 10^4$), the height of the plume is much larger, and consequently the local salinity and temperature differences at its top are larger. As a result the fluid in the annular region falls almost vertically and strong horizontal shears with high vorticity are produced between the upflow and the annular downflow and between the annular plume and the ambient fluid.

After the initial stage, a mixing-layer-type instability develops in the shear region between the annular plume and the ambient fluid. As a result of this instability, vortices form, which distort the outer boundary of the annular falling plume. The horizontal density gradient between the plume and the ambient fluid contributes to the vorticity and enhances the shear-generated vortices. The outer boundary of the plume becomes strongly convoluted and breaks down, and the annular plume becomes turbulent. We note, however, that the rising circular plume remains laminar during the whole observation time (about 3 h). An example of this sequence of events is shown in figure 4. We were not able to produce clear photographs of the vortices in the region between the annular falling plume and the ambient liquid (see, however, figure 4*g*), though these were clearly seen in the time-lapse pictures in all cases when the Rayleigh number was high enough.

4.2. *Double-diffusive layering*

As the turbulent annular plume develops, layers of three types form in a 'Christmas-tree' flow pattern (figure 5, plate 1). The layers of the first type (type I) form on top of the basic plume and are essentially the same as those developed in the case of small buoyancy flux mentioned above, since the warm top of the plume can be considered as heat source for the fluid situated above the plume. The type-I layers begin to form during the stage of instability and transition to turbulence of the annular plume, and are similar to those observed by Hubbel & Gebhart (1974) in the experiments on heating of a horizontal cylinder in a salinity gradient. A hierarchy of plumes forms successively on top of the basic one, which later develops into a system of (orange) layers. An example of this hierarchy is shown in figure 6 where more than ten successive secondary plumes can be seen. The number of layers in this hierarchy (at a particular time) depends upon the Rayleigh number in a surprisingly nonmonotonic manner. A maximum of this number was observed at Rayleigh number around 2×10^4. No systematic study of this phenomenon was made, since it was difficult to visualize the uppermost layers in our experiments.

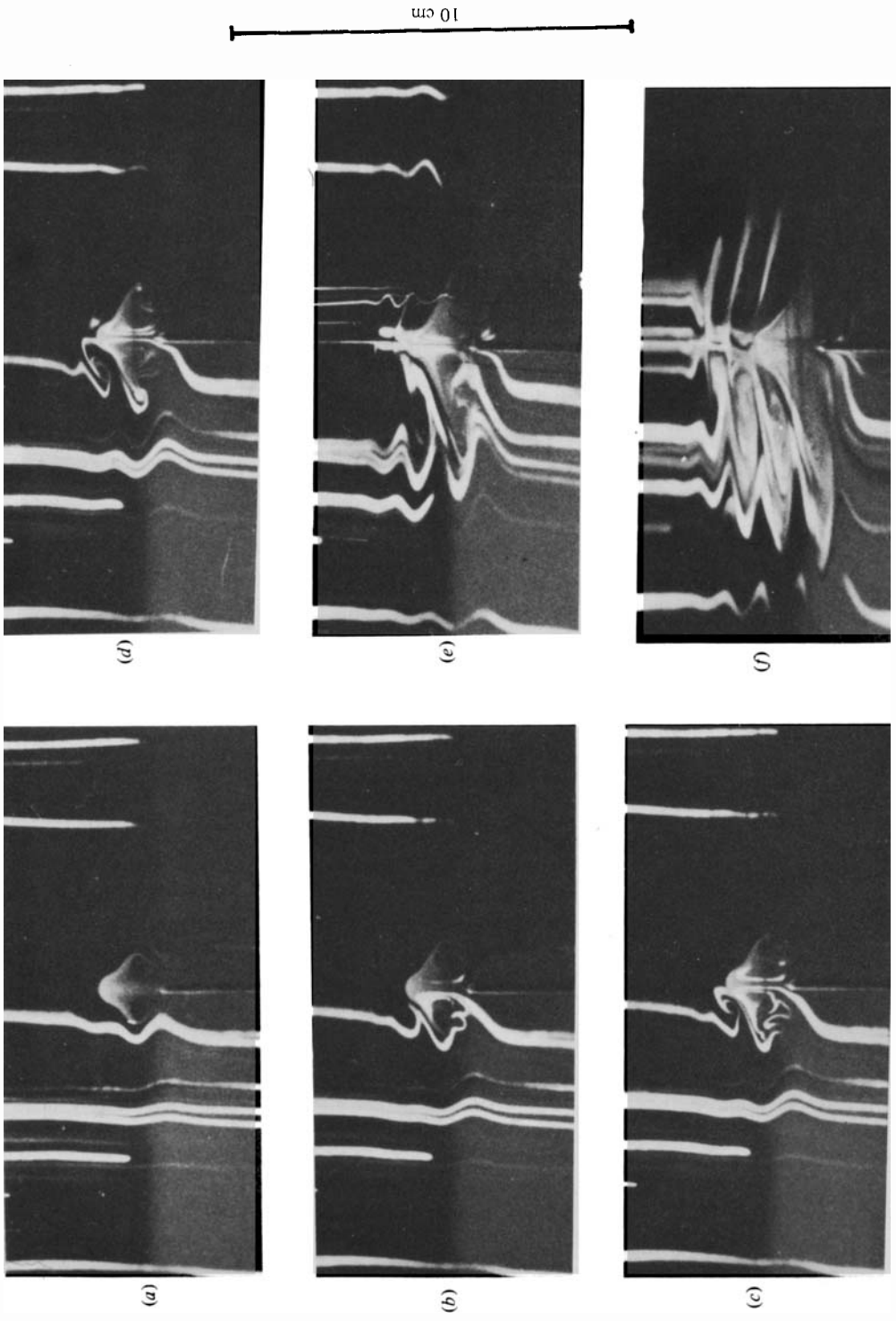

FIGURE 3. The laminar plume at $Ra = 5 \times 10^{-3}$: (*a*) $t = 37.2$ s; (*b*) 81.2 s; (*c*) 105.0 s; (*d*) 136.8 s; (*e*) 351.8 s; (*f*) 995.7 s (experiment no. 5, table 1).

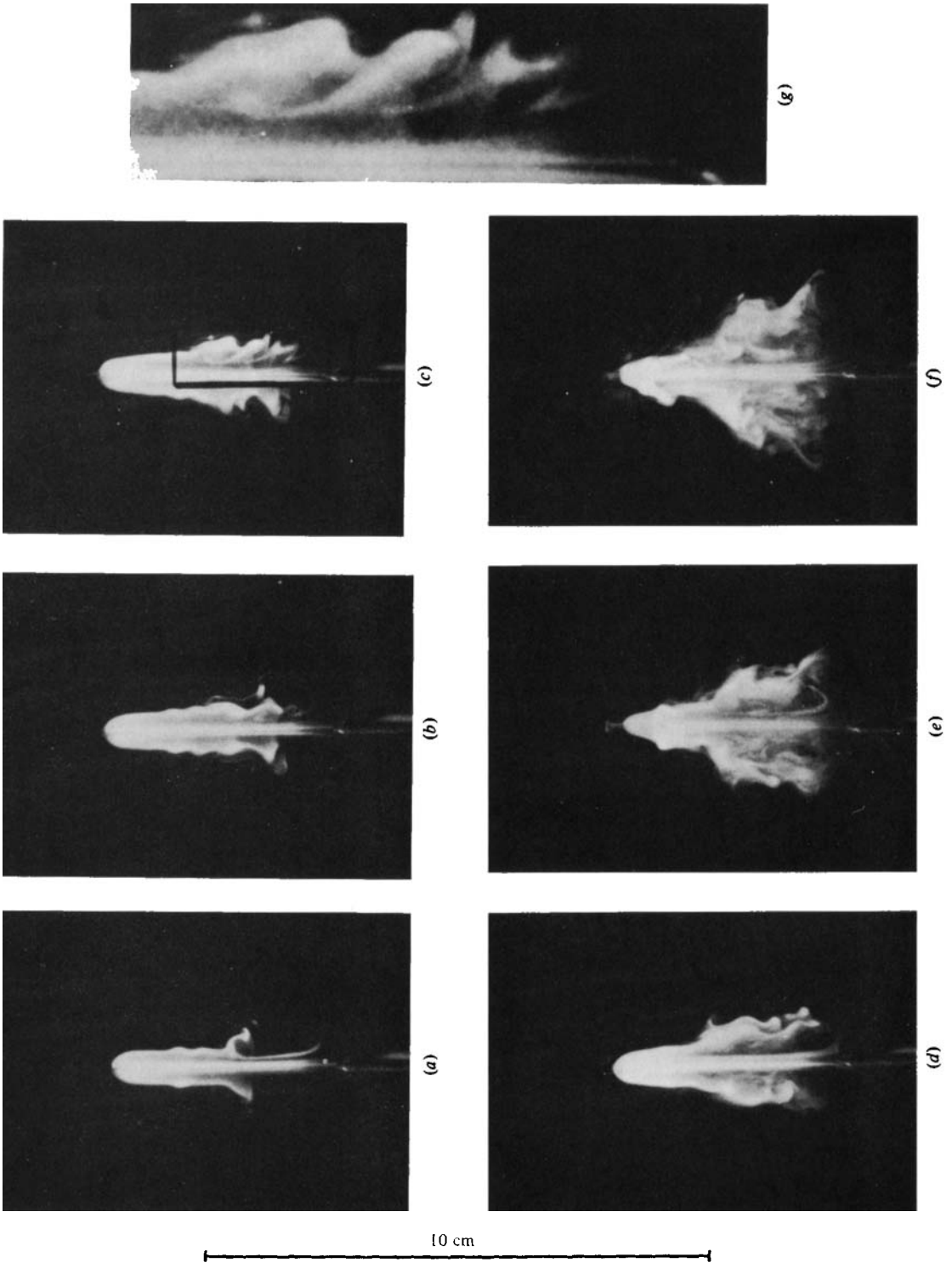
(g)
(c)
(f)
(b)
(e)
(a)
(d)
10 cm

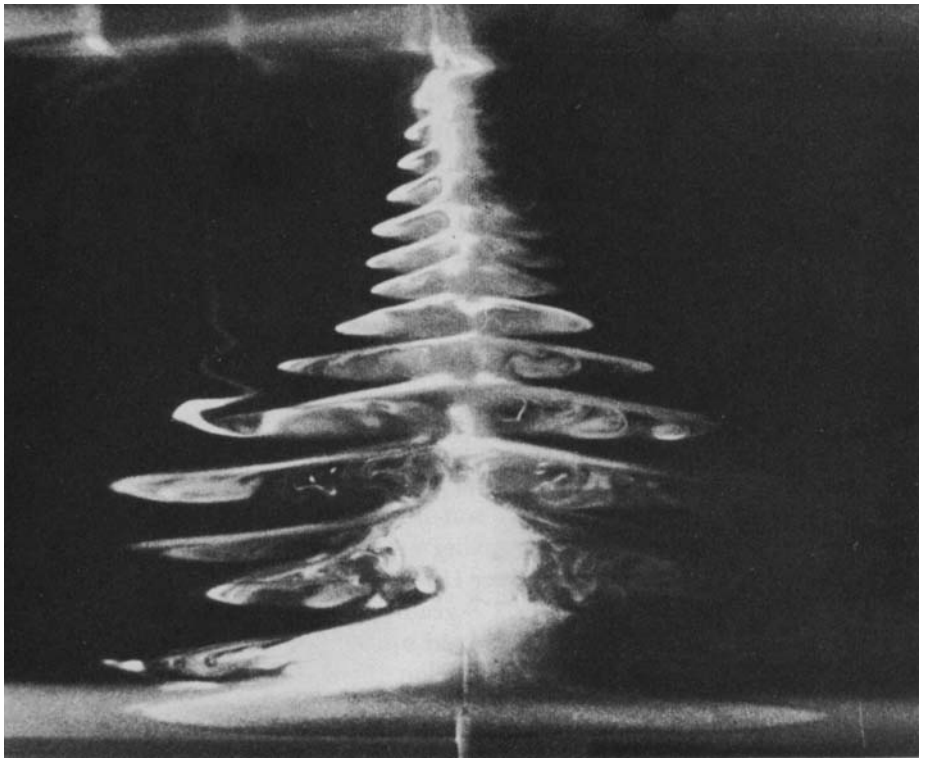

FIGURE 6. Hierarchy of type-I layers developed on top of the basic plume. $t = 2010$ s (experiment no. 9, table 1).

The layers of the second type (type II) are formed around the upper part (roughly one-third) of the basic plume. These layers are driven by the horizontal temperature difference between the warm basic plume and the cold ambient fluid. Therefore these layers are similar to those developing in the side-wall heating experiments described by Thorpe, Hutt & Soulsby (1969), Chen *et al.* (1971), Nekrasov, Popov & Chashechkin (1976), Popov & Chashechkin (1979) and Huppert & Turner (1980). In most cases, one layer of this type was formed.

Finally, the layers that we have called the third type form around the lower part of the basic plume. These layers are driven by the same mechanism as the layers of type II. However, they contain green (warmer and more saline) liquid, originating from the heat-source level, and in this respect are similar to the double-diffusive intrusions described by Turner (1978) and to the layers developing at fronts described by Ruddick & Turner (1979). In contrast with the number of the type-I layers the number of layers of types II and III together was independent of Ra and equal to three, and at larger times to four.

An example of these three types of layers is shown in figure 5 (*b*). It should be noted that the layers of the type I formed successively, whereas the layers of types II and III formed simultaneously. We note also that the distinction between the layers of

FIGURE 4. Instability and breakdown of the annular plume: (*a*) $t = 19.2$ s; (*b*) 26.0 s; (*c*) 38.0 s; (*d*) 54.0 s; (*e*) 94.3 s; (*f*) 149.8 s; (*g*) close up at $t = 38.0$. Note the vortices at the right-hand side of the annular plume in (*g*). (Experiment no. 3, table 1.) The scale refers to (*a*)–(*f*) only.

type II and III is somewhat arbitrary, since in a few cases we observed some green liquid in the layers classified as layers of type II.

When the Rayleigh number is larger than 10^5, the upper part of the circular plume is no longer stationary and oscillates around the centre (though the rising circular plume remains laminar). As a result of this, instead of forming an annular plume, the falling fluid (originating from the heat source level) forms a large annular body around the basic plume (figures 7*a*, *b*). At first sight this region seems to be mixed homogeneously almost everywhere. However, at later stages it splits into layers (figure 7*d*), which indicated that this region was stirred and mixed only partially, so that the fluid particles became distributed in the vertical according to the degree to which they were mixed with the ambient fluid.

4.3. *The layer structure*

The layers of all three types consist of a mixed upper region (orange for types I and II and green for type III), and of a non-mixed dark lower region. The dark lower region consists of the ambient fluid, which moves slightly upwards towards the warm plume where it becomes lighter and flows out into the interior as the mixed upper region of the layer. Thus 'systematic shearing motions are set up in both recently formed noses and established layers' (Turner 1978), which is the motion characteristic of layers formed by horizontal (lateral) T, S gradients.

The shearing flow extends beyond the mixed upper regions of the layers into the ambient fluid, which is seen from the deformation of the dye streaks shown in figure 5(*c*). This is generally attributed to the upstream influence produced by internal waves with small vertical wavelength (Turner 1978).

In addition to the radial motions, systematic azimuthal shearing motions are observed in the layers. The sense of the motions in the mixed upper part of the layer is opposite to the one in the lower dark part of the layer. In addition, the sense of these motions at a fixed level is not the same for different polar angles, which indicates the existence of horizontal cells. No azimuthal motions are observed beyond the mixed upper regions of the layers (and corresponding dark regions) in the ambient fluid, where radial motions still persist. At this stage we have not been able to develop an appropriate visualization technique for these motions, which were observed simply by dropping a dye particle and following the development of their traces. An example of this kind of observation is shown in figure 5(*b*). Examining the second trace from the left, one can see that the left part of this trace is dark, since it is moving away from the observer and the right one is bright, since it is moving in the opposite direction.

Another important feature of the structure of both type-I and type II layers is that the upper region of the layers consists of a system of vortices or rolls, an example of which is shown in figure 8. This picture is produced using small particles (of about 3 μm in diameter) dyed with a fluorescent dye. The time-lapse motion-pictures observation shows clearly that the vortices in the layers of type II are created near the plume when the dark lower part of the layer approaches the plume, and then are advected away from it. The vortices in the layers of type I are the caps of the secondary plumes separated from it and advected into the ambient fluid. The tilting of the type-I and II layers is due to double-diffusive convection driven by the buoyancy flux across the diffusive interfaces, separating the mixed part of one layer and the non-mixed part of the next layer above it (Huppert & Turner 1980). The creation of the vortices is due to heating of the approaching ambient fluid in the lower nonmixed part of the layers and to strong horizontal velocity gradients near the plume

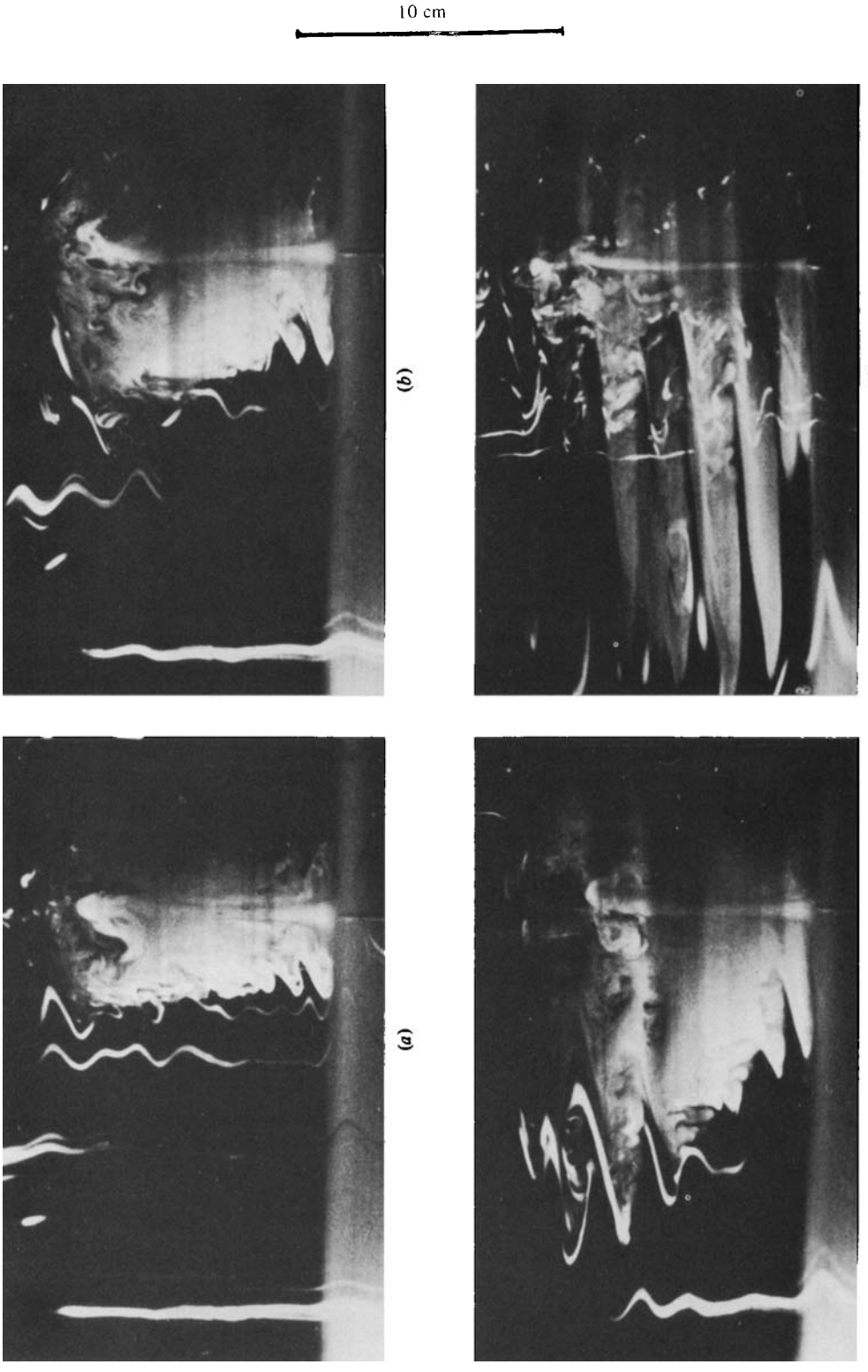

FIGURE 7. The splitting of the stirred annular plume into layers: (*a*) $t = 350.6$ s; (*b*) 590.6 s; (*c*) 1118.6 s; (*d*) 3108.0 s (experiment no. 12, table 1).

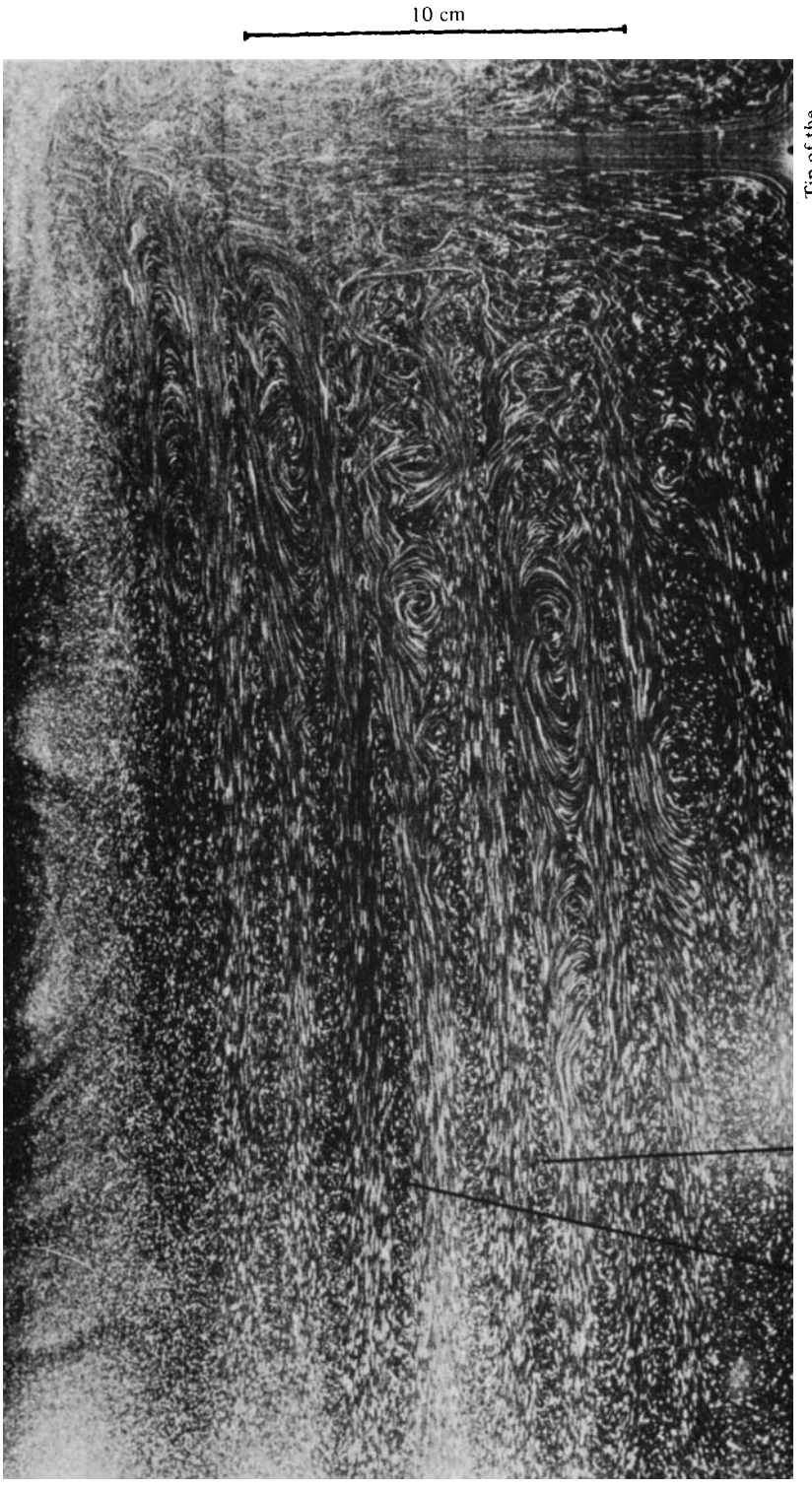

FIGURE 8. Flow structure in double-diffusive layers; $t = 1830$ s (experiment no. 4, table 1). Time exposure 5 s.

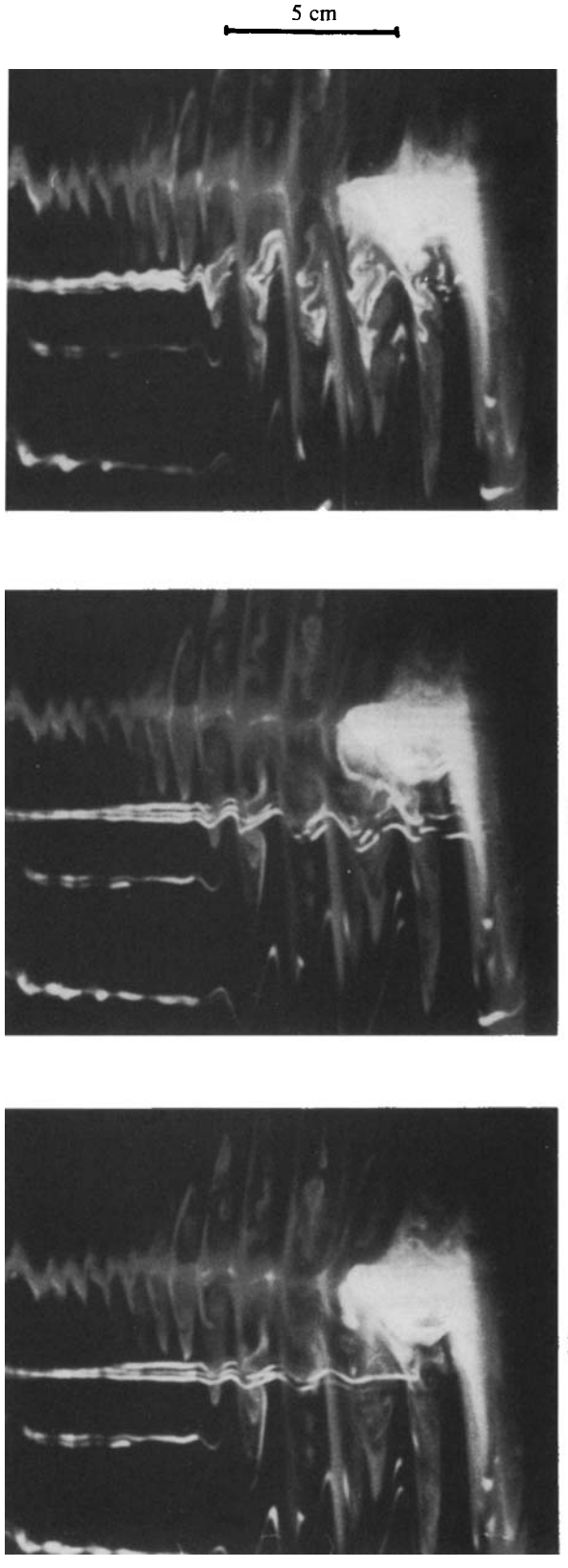

FIGURE 9. An example showing the motions within a layer: (*a*) shortly after dropping a dye particle; (*b*) 12 s later – systematic shearing motions; (*c*) 25 s after – vortical motions (experiment no. 9).

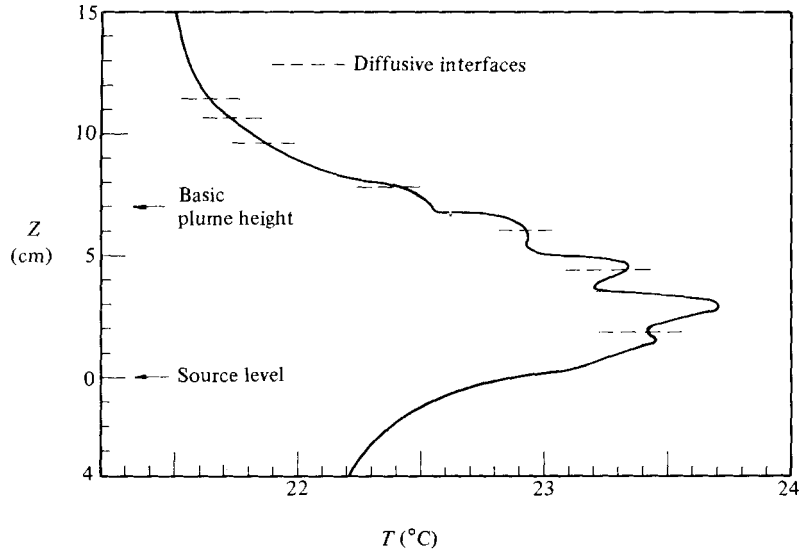

FIGURE 10. The temperature profile at $\Gamma = 4$ cm from the source; $t = 2400$ s (experiment no. 2, table 1).

core. Both causes contribute to vorticity in the same sense. Once created, these vortices do not become passive after leaving the plume. They become independent of the basic plume, but remain active, being driven by the following processes, which were deduced from the observation of dye streaks (e.g. figure 9).

The first one is the shear across the interface between the mixed upper part of the layer moving away from the plume, and the lower nonmixed part of the layer moving toward the plume. The second is the upward buoyancy flux due to the negative temperature gradient (see figure 10), which is produced by the larger horizontal heat flux in the lower layers. The third factor tending to drive motions in the same sense is the horizontal density gradient. In other words, the vortices are the manifestation of the vorticity produced by these three factors.

The layers of type III are similar to the intrusions extensively studied by Turner (1978). In his terminology these are S-intrusions into an S-gradient (with different T, however). It is typical that fluid from the basic plume originating from the heat source level is intruding into the ambient fluid to form these layers (this was the reason why these layers were green). Therefore there is an excess of salt and temperature in these layers (see figure 10), so that diffusive interface forms above the intrusion and fingers below it, as shown in figure 5. The slight downward tilting of the green layers implies that the net buoyancy flux into the intrusion through the diffusive and finger interfaces is negative. It is worth noting that in the case of an S-intrusion into a T-gradient the tilting was upwards (Turner 1978). In the layers of type III, vortex-like motions also existed, although they were smeared out by the salt fingers.

4.4. *The height of the plume and vertical lengthscale of the layers*

In figure 11 are shown the non-dimensional height of the basic plume H/l_{FN} and the vertical lengthscale h/l_{FN} of the layers of type II and III, which appeared to be of the same vertical scale within the accuracy of the experiments, versus Rayleigh number. The parameters and results are presented in table 1. The data used are the

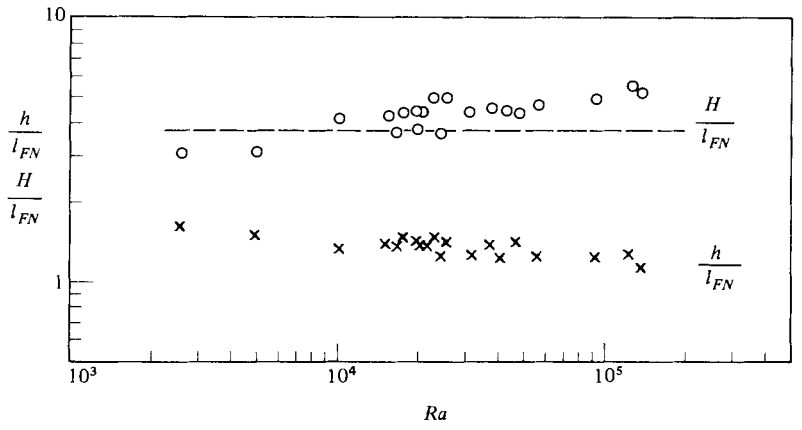

FIGURE 11. The non-dimensional height of the basic plume H/l_{FN} (○) and layer 'thickness' h/l_{FN} (×) as functions of the Rayleigh number. The dotted line corresponds to the value 3.76 for the turbulent plume in a one-component stratified fluid.

Experiment no.	Q (W)	F (cm^4/s^3)	N (s^{-1})	l_{FN} (cm)	H (cm)	h (cm)	H/l_{FN}	h/l_{FN}	$Ra \times 10^{-4}$
1	2.24	0.158	0.618	0.90	3.9	1.3	4.38	1.44	1.78
2	5.93	0.416	0.618	1.15	5.0	1.6	4.35	1.39	4.70
3	3.94	0.276	0.618	1.04	4.5	1.3	4.3	1.25	3.11
4	4.80	0.337	0.618	1.09	4.9	1.5	4.5	1.38	3.81
5	0.63	0.044	0.618	0.66	2.0	1.0	3.03	1.52	0.50
6	2.89	0.203	0.618	0.96	4.8	1.4	5.00	1.46	2.30
7	2.70	0.190	0.618	0.95	4.3	1.3	4.52	1.37	2.14
8	3.28	0.23	0.618	1.00	5.0	1.4	5.0	1.4	2.60
9	1.00	0.070	1.234	1.53	6.8	2.1	4.44	1.37	2.09
10	4.40	0.309	1.07	0.71	2.7	1.0	3.8	1.41	2.02
11	0.64	0.045	0.206	1.51	6.4	2.1	4.24	1.39	1.52
12	8.86	0.622	0.347	1.92	10.6	2.4	5.52	1.25	12.20
13	0.41	0.029	0.119	2.03	7.6	2.8	3.74	1.38	1.69
14	1.77	0.124	0.357	1.28	4.6	1.6	3.6	1.25	2.43
15	1.29	0.091	0.618	0.795	3.2	1.1	4.05	1.39	1.02
16	6.98	0.490	0.618	1.20	5.6	1.5	4.67	1.25	5.54
17	6.79	0.476	0.357	1.80	8.8	2.2	4.88	1.22	9.30
18	1.95	0.137	0.234	1.81	7.8	2.2	4.32	1.22	4.10
19	17.18	1.205	0.618	1.50	7.9	1.7	5.26	1.13	13.60
20	0.19	0.0134	0.357	0.74	2.3	1.2	3.10	1.62	0.26

TABLE 1. The experimental parameters and results of the experiments on a heat source in a salinity gradient

means of at least 20 individual values measured at 5 (or more) times for the 3–4 layers of types II and III, after the layers were developed enough.

There seems to exist a very weak dependence of H/l_{FN} and h/l_{FN} on Ra, but it is barely significant and at this stage we suggest that both H/l_{FN} and h/l_{FN} be assumed constant in the explored range of Ra. Correspondingly, $H/l_{FN} = 4.4 \pm 0.6$ and $h/l_{FN} = 1.3 \pm 0.25$. Note that the average value for H/l_{FN} is about 20% larger than the value for the turbulent-plume height in a one-component stratified fluid, which is $5.0\pi^{-\frac{1}{4}} = 3.76$ (Turner 1973). We shall return to this point in §5. At large

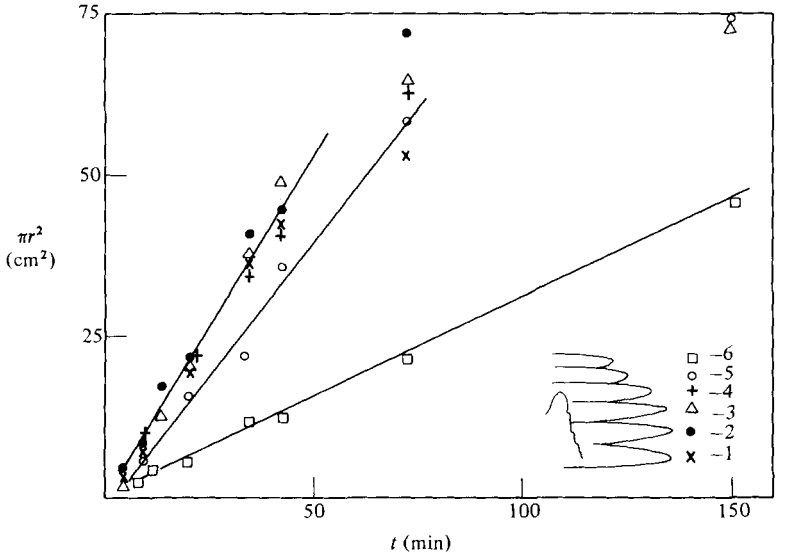

FIGURE 12. Time dependence of layer area πr^2 (r = layer radius) (experiment no. 4, table 1).

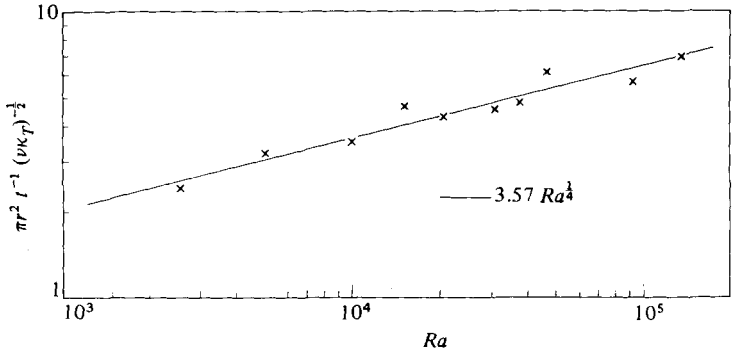

FIGURE 13. The non-dimensional rate of lateral spreading $\pi r^2 t^{-1} (\kappa_T \nu)^{-\frac{1}{2}}$ for layers of type II and III, as a function of the Rayleigh number. The solid line is $3.5Ra^{\frac{1}{4}}$.

times, especially when the layers of type III reached the sidewalls of the tank, the height of the basic plume was observed to increase slightly.

4.5. *The horizontal development of the layers*

The rate of lateral spreading of a layer should depend on its vertical distance from the heat source. However, the layers of type II and III developed within 10% at the same rate and only the rate of spread of the type-I layers exhibited this dependence. This is clearly seen from figure 12, where the area of the layers is plotted versus time. It is clear also from this figure that up to some limit the areal rate of spread of the layers is constant and it is believed that the change in this rate is due to the influence of the sidewalls of the tank. The dependence of the layers' rate of spread on Rayleigh number is of special interest, since it provides some indication of the dependence of horizontal heat and salt fluxes on Rayleigh number. This dependence is shown in figure 13, which indicates that the rate of the areal spread is proportional to $Ra^{\frac{1}{4}}$.

These results† should be considered as preliminary, since a considerable degree of uncertainty existed in the measurements of the layers' lateral extent.

5. Discussion and concluding remarks

The scales of the basic plume and layers. At this stage we are unable to make a direct comparison with the result of the sidewall heating experiments (Chen, Briggs & Wirtz 1971; Huppert & Turner 1980) and experiments on layering at a T, S front (Ruddick & Turner 1979), since no systematic temperature measurements were made. However, the consistency of our results with those mentioned above can be checked to some extent qualitatively in the following way. Let ΔT be the temperature difference imparted to fluid particles at the heat source. The height of the basic plume cannot exceed the value of $2\alpha\Delta T/(\beta\,\mathrm{d}S/\mathrm{d}z)$, which is the height of plume rise without losing energy, heat and salt. Under such conditions, at the height $\alpha\Delta T/(\beta\,\mathrm{d}s/\mathrm{d}z)$ (which is the level where the density of fluid particles is equal to the density of the ambient fluid), the particles acquire the kinetic energy to be able to overshoot to the same height.

On the other hand, we have some indications that the temperature change in the plume along its height is not large (about 20 % of the total). The fact that the vertical lengthscale of type-II and -III layers and their rate of horizontal spread are independent of height along the plume provides support for this assumption. Thus, as a crude estimate, the temperature difference between the hot plume and the ambient fluid could be assumed to be equal to ΔT, where ΔT is the value mentioned above. Therefore the vertical lengthscale of the layers could be estimated as 0.6–$0.7\alpha\Delta T/(\beta\,\mathrm{d}S/\mathrm{d}z)$ (Ruddick & Turner 1979; Huppert & Turner 1980).‡ Thus, about three layers are expected to form along the height of the basic plume. This is what was observed in our experiments at earlier stages of the 'Christmas-tree' development. However, at a later stage, up to four layers were observed along the height of the plume.

Another point deserving comment is that the height of the basic plume is $4.4F_1^{\frac{1}{4}}N^{-\frac{3}{4}}$, which is about 20 % larger than for a turbulent plume in a single-component stratified fluid. The possible reason for this relation is that in our experiments the central circular plume was not turbulent although the annular one was, provided that $Ra \geqslant 10^4$. This question is not resolved and further work is necessary to clarify this point, especially at larger Rayleigh numbers when the whole plume is turbulent. This is of special interest also in the context of the splitting of the stirred annular region into layers, described in §4.

The hierarchy of secondary plumes. The existence of a maximum in the number of the secondary plumes indicates that a maximum in the vertical heat flux should exist. On the other hand, the $Ra^{\frac{1}{4}}$ dependence of the horizontal spread of the layers indicates that the horizontal heat flux should increase with Ra. These conjectures are another point for further study.

The layer structure. As described above, we observed some features of the structure of individual layers. The layers consisted of a mixed upper region moving away from

† A table of the detailed parameters and results used in preparing figure 13 has been deposited with the editorial office of the journal, from where interested readers may obtain copies.

‡ The typical temperature difference ΔT and the initial density gradient $(1/\rho_0)\,\mathrm{d}\rho/\mathrm{d}z$ in our experiments were of order 10 °C and 5–10^{-4} cm^{-1} so that the Rayleigh number as defined in Huppert & Turner (1980) was of order 10^7. This justifies the choice for the coefficient 0.6–0.7 in the estimate for the vertical scale of the layers.

the plume and non-mixed lower region of ambient fluid moving towards the plume and forming in this manner a systematic radial shearing motion. The upper mixed region of the layers contained vortices and in addition the layers of type III contained salt fingers. The most intriguing features of the layer structure observed in our experiments were the systematic azimuthal shearing motions (in addition to radial ones). At this stage we don't understand how they arise and what is the mechanism that produces this kind of motion. One may speculate that it is likely to be the result of an instability of the axisymmetric flow with respect to a θ-dependent mode (where θ is the azimuthal angle) but further work is necessary to resolve this problem.

The authors are grateful to Professor J. S. Turner and Dr H. E. Huppert for their interest in this work and useful discussions during the conference on double-diffusive convection in Santa Barbara (13–18 March 1983, Engineering Foundation Conference), which contributed a lot to the final version of the paper. We thank Mr J. Tanny whose help made it possible to produce figure 8. We wish also to express our appreciation of the referees' comments, which aided the improvement of the manuscript.

Note. After this work was submitted for publication Professor R. E. Kelly drew the attention of one of the authors (A.B.T.) to the papers of Chashechkin & Tupitsyn (1979) and Tupitsyn & Chashechkin (1981) describing similar experiments. Their work and ours are the complement of one another.

REFERENCES

Chashechkin, Y. D. & Tupitsyn, V. S. 1979 Structure of free convective flow above a point source of heat in a stratified liquid. *Sov. Phys. Dokl.* **24**, 862–864.

Chen, C.F., Briggs, D. G. & Wirtz, R. A. 1971 Stability of thermal convection in a salinity gradient due to lateral heating. *Intl J. Heat Mass Transfer* **14**, 57–65.

Fischer, H. 1971 The dilution of an undersea sewage cloud by salt fingers. *Water Res.* **5**, 909–915.

Hubbell, R. H. & Gebhart, B. 1974 Transport processes induced by a heated horizontal cylinder submerged in quiescent salt-stratified water. In *Proc. 1974 Heat Transfer and Fluid Mechanics Institute*, pp. 203–219.

Huppert, H. E. & Linden, P. F. 1979 On heating a salinity gradient from below. *J. Fluid Mech.* **95**, 431–464.

Huppert, H. E. & Turner, J. S. 1980 Ice blocks melting into a salinity gradient. *J. Fluid Mech.* **100**, 367–384.

Huppert, H. E. & Turner, J. S. 1981 Double-diffusive convection. *J. Fluid Mech.* **106**, 299–329.

Nekrasov, V. N., Popov, V. A. & Chashechkin, Yu. D. 1976 Formation of a periodic convective flow structure during lateral heating of a stratified fluid. *Bull. Acad. Sci. USSR, Atmos. Oceanic Phys.* **12**, 733–739.

Paliwal, R. C. & Chen, C. F. 1980 Double-diffusive instability in an inclined fluid layer. Part 1. Experimental investigation. *J. Fluid Mech.* **98**, 755–768.

Popov, V. A. & Chashechkin, Yu. D. 1979 On the structure of thermohaline convection in a stratified fluid. *Bull. Acad. Sci. USSR, Atmos. Oceanic Phys.* **15**, 668–675.

Ruddick, B. R. & Turner, J. S. 1979 The vertical length scale of double-diffusive intrusions. *Deep-Sea Res.* **26**, 903–913.

Sherman, F. S., Imberger, J. & Corcos, G. M. 1978 Turbulence and mixing in stably stratified water. *Ann. Rev. Fluid Mech.* **10**, 267–288.

Shlien, D. J. & Thompson, D. W. 1975 Some experiments on the motion of an isolated laminar thermal. *J. Fluid Mech.* **72**, 35–47.

Thorpe, S. A., Hutt, P. K. & Soulsby, R. 1969 The effect of horizontal gradients on thermohaline convection. *J. Fluid Mech.* **38**, 375–400.

TUPITSYN, V. S. & CHASHECHKIN, YU. D. 1981 Free convection above a point source of heat in a stratified fluid. *Izv. Akad. Nauk SSSR, Mekh. Zhid. i Gaza* no. 2, 27–36.

TURNER, J. S. 1973 *Buoyancy Effects in Fluids.* Cambridge University Press.

TURNER, J. S. 1974 Double-diffusive phenomena. *Ann. Rev. Fluid Mech.* **6**, 37–56.

TURNER, J. S. 1978 Double-diffusive intrusions into a density gradient. *J. Geophys. Res.* **83**, 2887–2901.

TURNER, J. S. 1979 Laboratory models of double-diffusive processes in Ocean. In *Proc. 12th Symp. Naval Hydr., Washington D.C.*, pp. 596–606.

TURNER, J. S., & CHEN, C. F. 1974 Two-dimensional effects in double-diffusive convection. *J. Fluid Mech.* **63**, 577–592.

TURNER, J. S. & GUSTAFSON, L. B. 1978 The flow of hot saline solutions from vents in the sea floor – some implications for exhalative massive sulfide and other ore deposits. *Econ. Geol.* **73**, 1082–1100.

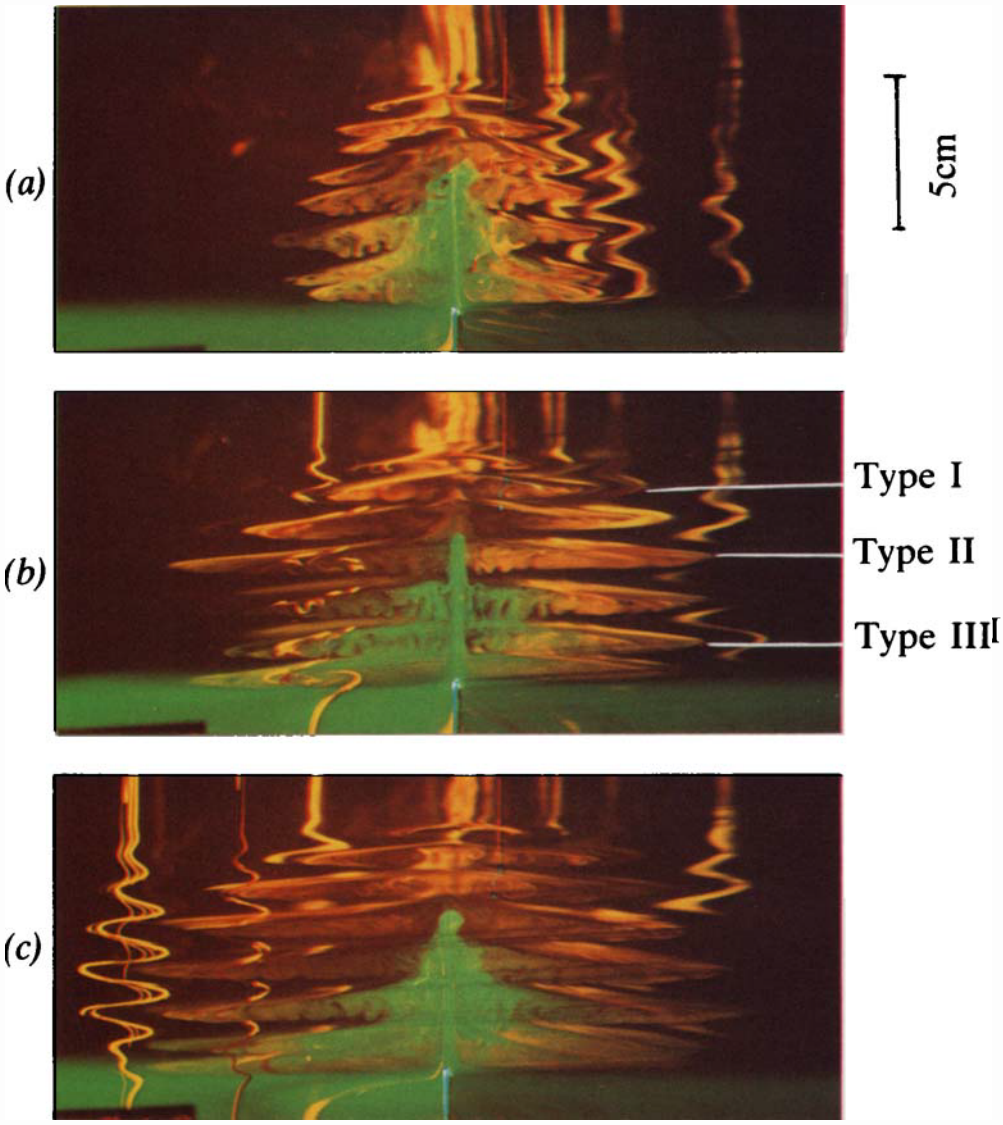

FIGURE 5. Christmas-tree flow pattern of layer formation: *(a)* $t = 520.9$ s; *(b)* 1126.7 s; *(c)* 1596.0 s (experiment no. 4, table 1).